



# Mass-production of boron nitride double-wall nanotubes and nanococoons

John Cumings, A. Zettl \*

*Department of Physics, University of California at Berkeley, and Materials Sciences Division, Lawrence Berkeley National Laboratory, Berkeley, CA 94720, USA*

Received 4 October 1999; in final form 22 October 1999

## Abstract

Various techniques including plasma-arc, laser ablation, and chemical vapor-phase synthesis have been employed to produce bulk amounts of non-carbon (such as boron nitride, BN) nanotubes with some success, but in general the yields are low. We describe a new high-yield plasma-arc method that easily and reliably produces macroscopic amounts of pure BN nanotubes. Interestingly, the method produces almost exclusively double-walled nanotubes; these in turn self-assemble into BN nanotube bundles or ropes. Our synthesis method also produces BN-coated crystalline nanoparticles, whose cores can be preferentially etched leaving behind hollow BN ‘nanococoons’. © 2000 Elsevier Science B.V. All rights reserved.

## 1. Introduction

Carbon nanotubes have been the subject of intense recent interest because of their unique electronic, thermal, and mechanical properties. Equally interesting are non-carbon nanotubes. Compounds with a propensity for graphite-like layering are natural candidates for nanotube formation, and indeed transition-metal dichalcogenides and hexagonal boron-nitride based nanotubes have been variously predicted [1] and observed [2–9]. Importantly, some of the predicted properties of non-carbon nanotubes are, for certain applications, superior to those of pure carbon nanotubes. For example, BN nanotubes are predicted [10] to have a uniform electronic bandgap independent of the diameter and chirality of the tube,

and thus, in contrast to multi-walled carbon tubes, multi-wall BN nanotubes are electronically ‘uniform’. Unfortunately there is no reliable method to produce bulk amounts of such non-carbon nanotubes. Several techniques including plasma-arc [6–9], laser techniques [3,4], and chemical vapor-phase synthesis [2,5,11] have been employed with some success, but consistently the yields are disappointingly low.

One of the simplest methods to produce bulk quantities of carbon nanotubes involves the arcing of graphite electrodes in an inert atmosphere [12]. This efficient method unfortunately cannot be directly applied to the synthesis of boron-nitride nanotubes since BN is electrically insulating and forms an unsuitable arcing electrode. Various methods have been developed to circumvent this problem. They include packing the insulating BN into a metal casing for arcing [7], or arcing conducting metal borides in a nitrogen atmosphere [9]. These methods neces-

\* Corresponding author. Fax: +1-510-643-8497; e-mail: azettl@physics.berkeley.edu

sarily result in an abundance of metal atoms in the growth plasma. While some amount of metal may be beneficial and serve as a tube formation catalyst, an overabundance of metal may actually hamper tube growth.

We here describe a new high-yield non-equilibrium plasma-arc method that easily and reliably produces macroscopic amounts of pure BN nanotubes. The method allows for a controllable and relatively low metal content in the growth reactants and produces almost exclusively double-walled nanotubes in high yield. The double-walled BN nanotubes in turn self-assemble into nanotube bundles or ropes. Our synthesis method also produces BN-coated crystalline nanoparticles, whose cores can be preferentially etched leaving behind hollow BN ‘nanococoons’. For a given set of synthesis conditions, the nanoparticles and associated nanococoons size distribution can be made nearly monodisperse.

## 2. Synthesis

The synthesis method employs nitrogen-free, boron-rich conducting electrodes arced in a pure nitrogen gas environment. The electrodes incorporate only a small amount of nickel and cobalt, used primarily as a catalyst. The electrodes are formed by first intimately mixing elemental boron (99 + % pure) with 1 atomic percent each of nickel and cobalt. The mixed powder is then heated to melting in a commercial copper-hearth arc furnace, and cooled to form a macroscopically homogenous ingot. We achieve equivalent results by melting separate boron, nickel and cobalt ingots together in the same hearth. The ingots have no well-defined shape, but are typically approximately 1 cm × 1 cm × 2 cm. Using a crude two-probe method, the electrical resistivity of the ingots is measured to be less than 50 milliohm-meters. When the boron ingots are formed without the addition of metal, they are not conducting enough to support the arc. The ingots themselves are mounted as both anode and cathode in a conventional-design water-cooled nanotube direct-current arc synthesis chamber. The electrodes are mounted vertically with the anode being the top electrode. The chamber is pumped down to less than 30 mtorr and then back-filled with N<sub>2</sub> gas with the pressure dynamically

stabilized to 380 torr. During a synthesis run the arc current is sustained nominally at 60 amperes DC with electrode voltage in the range 30 to 45 V.

During the arc, a gray web-like material grows preferentially near the top of the chamber, while a thin layer of gray soot covers the side walls of the chamber. Both the web-like material and the gray soot contain an abundance of BN nanotubes, but the web-like material is significantly richer in BN nanotubes. Samples of raw material removed from the chamber are ultrasonically dispersed in isopropanol and evaporated onto holey carbon grids for characterization with a Topcon EM-002B transmission electron microscope (TEM), operating at 200 kV or 100 kV accelerating voltage.

## 3. Results and discussion

Fig. 1 shows a typical TEM image of a BN nanotube, whose source was the web-like material. We interpret the dark bands in the figure as representing the two concentric cylinders of a two-walled nanotube. The two concentric shells of this particular specimen have inner and outer diameters of 2.2 nm and 2.9 nm, respectively, leading to an interwall spacing of about 0.37 nm. The inset to Fig. 1 shows the end of a different BN nanotube. Interestingly, there is no evidence for a catalytic particle at the end of the tube. Indeed, on this tube there does not appear to be a cap of any kind (i.e. the tube is open-ended). This may have implications for the growth mechanism of BN nanotubes using a nickel/cobalt catalyst. Because of the relatively long length of the BN nanotubes produced by our synthesis method (at least many microns), we are able to observe the ends of tubes only infrequently in the TEM. It is therefore unknown if all the tubes produced are open-ended. As will be discussed shortly, electron energy loss spectroscopy studies confirmed the expected BN stoichiometry of the nanotubes.

The double-walled nanotube shown in the main body of Fig. 1 is representative of nearly all nanotubes generated by our plasma arc-runs (although, as will be discussed below, such tubes often organize into bundles or ‘ropes’). Importantly, virtually all of the BN nanotubes are double-walled. Fig. 2 shows the observed distribution of number of walls for our

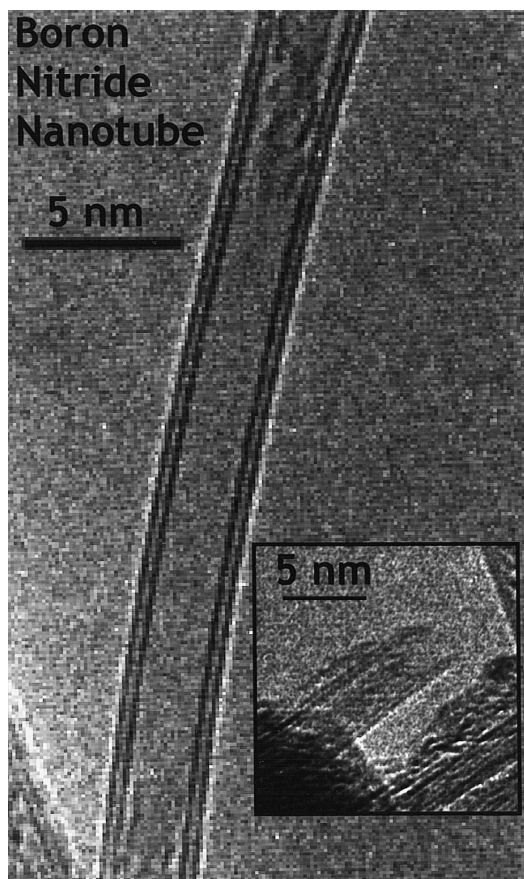


Fig. 1. High resolution TEM image of a BN nanotube with two layers. Inset: Image of a BN nanotube end.

BN nanotubes, obtained from visually counting tubes during TEM imaging. Similar data are obtained from different TEM grid preparations. The distribution is strikingly and sharply peaked at two walls. No nanotubes with wall numbers other than those indicated in the histogram were observed.

Additional statistics were obtained for the abundant double-walled tubes. The tubes have a narrow diameter distribution, centered about 2.7 nm (outer diameter), with a standard deviation of 4 Å. The distance between the outer wall and the inner wall is  $3.6 \pm 0.3$  Å. Interestingly, this value appears slightly larger than the 3.33 Å interlayer spacing expected for flat hexagonal BN [13].

In order to verify the composition of the BN nanotubes, we performed electron energy loss spectroscopy (EELS). We used a Gatan 666 EELS spec-

trometer installed in a JEOL JEM 200CX TEM, operating at 200 kV accelerating voltage. The EELS spectra obtained on individual nanotubes and bundles of nanotubes suspended over holes in the grid show characteristic boron and nitrogen K edges at 188 eV and 401 eV, respectively. Notably absent is the 284 eV carbon K edge, which was observed readily using the holey carbon grid itself as a reference. The stoichiometry of the nanotube is calculated from weighted intensity of the resulting spectrum, with an error due to background subtraction of typically  $\sim 20\%$ . The N:B ratios calculated for our spectra range from 0.7 to 1.2, indicating that within experimental error the BN nanotubes have the approximate atomic ratio B:N = 1:1.

Additional features of the TEM imaging deserve further comment. First, although the interiors of the tubes appear for the most part ‘hollow’, there are observed numerous regions where the tubes seem to be partially filled with amorphous material. Exam-

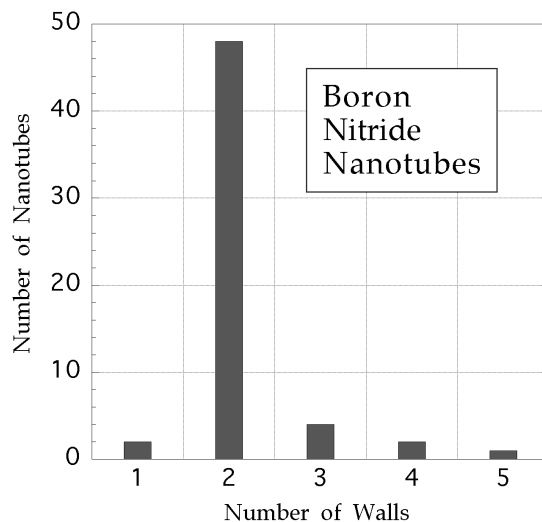


Fig. 2. Histogram of BN nanotube wall number. The present synthesis method yields almost exclusively double-walled nanotubes.

ples of such partial filling can be seen in the upper and lower portions of the main body of Fig. 1. We have observed no systematic differences in the EELS spectra of hollow and partially filled regions of the tube, suggesting that the filling material may be amorphous BN. Only much less frequently is any amorphous material observed attached to the outside of the tube walls (i.e. in general the outer surfaces of tubes are quite clean). In certain instances, the tube filling assumes a vague structure that can even appear like an ill-formed third inner wall, sometimes with an intensity modulation along the tube length. The effect is reminiscent of the modulation observed in some preparations of single-walled carbon nanotubes, where the modulation has been interpreted as originating from (mobile)  $C_{60}$  units [14].

Another important feature of the long, clean, nearly monodisperse BN nanotubes produced by our synthesis method is their propensity to align with each other and form bundles or ropes. Fig. 3a shows a TEM image of a bundle of (in this case three) double-wall BN tubes. These bundles extend for at least several hundred nanometers, eventually becoming obscured by other similar bundles in the TEM images. The organized bundling of these nanotubes is similar to that observed in preparations of high-quality single-walled carbon nanotubes [15].

To better characterize the length of the BN nanotube bundles, we examined our samples with a scanning electron microscope (SEM). The samples were coated with  $\sim 30$  nm of gold before loading into a Gemini Leo SEM. Samples which are not first coated with gold display detrimental charging effects, reflecting the insulating nature of BN nanotubes. Fig. 3b shows a SEM image of the raw web-like material taken from the arc synthesis chamber. The image reveals many fibers with diameters from 10–50 nm. The fibers are intermixed with amorphous-looking nodules, and often stretch well beyond  $2 \mu\text{m}$  between connections. These bundles or ropes of nanotubes are found in soot from all portions of the arc chamber, but are more abundant in the web-like material, consistent with our TEM analysis.

The amorphous-looking nodules observed in the SEM image of Fig. 3b are not strictly amorphous, but have an internal structure. They consist of clustered nanocrystals (tentatively identified from EELS

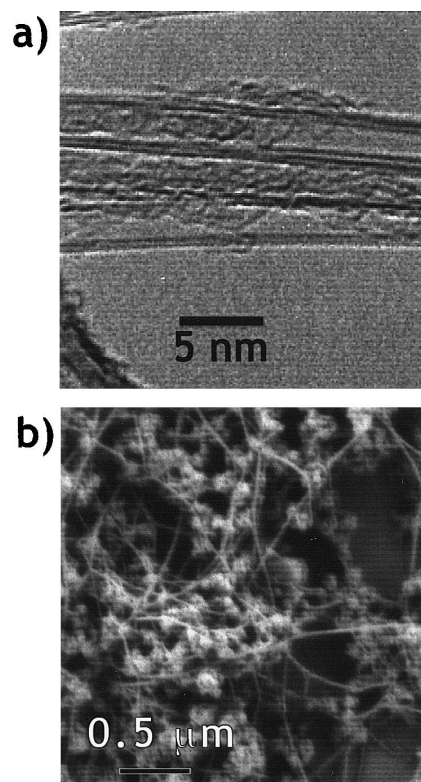


Fig. 3. (a) TEM image of BN nanotube bundle or rope. The bundle shown contains three double-walled nanotubes. (b) SEM image of BN nanotube ropes.

studies as pure boron), individually coated with multiple layers of graphite-like BN. Fig. 4a shows a high resolution TEM image illustrating the structure of the coated nanocrystals. The BN coating or cage is often well-crystallized into several layers. However, the BN coating is not perfectly spherical, nor does it always perfectly follow the contour of the internal nanocrystal. Rather, the cage has sharp facets, as expected from the in-plane bonding structure of hexagonal BN.

We have discovered a method of removing the nanocrystal interiors from the BN cage structures, leaving behind intact hollow BN ‘nanocoons’. The cluster-containing BN soot is added to concentrated nitric acid, and heated to near boiling. As the acid is heated, it evolves a noxious brown/orange gas, first slowly, then vigorously. After about 5 min, the evolution of gas slows and the soot is noticeably lighter in color. The solution is kept near boiling for

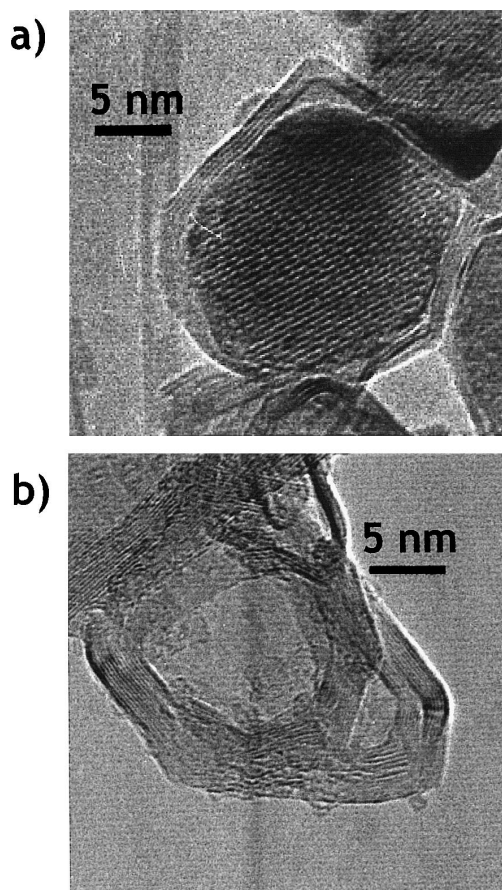


Fig. 4. (a) BN-coated boron nanocrystal. b) Same as (a), after treating with nitric acid. The boron has been chemically removed, leaving an empty BN nanococoon.

another 15 min, followed by rinsing in distilled water and then isopropanol. The treated material is then dispersed onto holey carbon grids from solution in the remaining isopropanol. Fig. 4b shows a TEM image of the BN nanococoon following removal of the core. Interestingly, the nitric acid treatment does not appear to adversely affect the BN cage structure, even where the BN layers are faceted or sharply strained. This begs the question of how the nanocrystal material actually escapes from the BN cocoon. We are uncertain if the BN cage contains a small initial or acid-induced perforation, or (less likely) if diffusion actually takes place through the closed cocoon fabric itself. In any case, TEM imaging reveals that the acid treatment hollows out nearly

100% of the BN cocoons. A reversible depletion/filling of chemically robust BN nanococoons with selected atomic or molecular species would have important technological implications in the chemical, or electrochemical, industries.

Finally, we comment on the growth mechanisms for BN nanotubes and ropes. We do not know what mechanism favors a two-walled structure. An understanding of such BN structures and the underlying kinetics could help to elucidate the growth mechanisms for BN (and carbon) nanotubes. The double-wall structure has been observed to form in the case of  $\text{HfB}_2$  arced in nitrogen gas [9], and is claimed to be the dominant structure in laser ablation of BN with Ni/Co catalyst carried out in nitrogen carrier gas [4]. It has been proposed that lip–lip interactions could stabilize the growth of open-ended multi-wall carbon nanotubes [16], and indeed we have indications that the two-walled BN nanotubes we observe grow open-ended. It is likely that the transition metals in the present synthesis method serve as a catalyst, preferentially producing nanotubes with small diameters, as they do in the case of single-wall carbon nanotubes [17,18]. It has been predicted that the B–N bond of a single-wall BN nanotube should naturally undergo out-of-plane buckling [10], producing a dipolar shell. This buckling may hinder the formation of a single-layered tube. Two-walls may help to stabilize the growth of BN nanotubes, in contrast to carbon which can grow efficiently with just a single wall (a more detailed histogram than that shown in Fig. 2 would be needed to ascertain if BN nanotubes with an even number of walls are generally favored). Additionally, the resistance of BN to forming pentagon defects may sustain the open ended growth. This efficient growth may account for the significant length of the BN nanotubes described here, giving the two-wall structure a majority when observed in bulk.

#### 4. Conclusion

Our successful synthesis of bulk quantities of double-walled BN nanotubes is significant in that it allows not only the study of bulk BN nanotube characteristics, but presents the unique opportunity to

examine experimentally nanotubes which have only two walls.

### Acknowledgements

We thank J. Wu for help in preparing the electrodes, and U. Dahmen and S. Chen for preliminary microscopy work. We acknowledge A. Edwards for technical assistance, and V. Crespi for useful discussions. This research was supported in part by the Director of the Office of Energy Research, Office of Basic Energy Sciences, Materials Sciences Division of the U.S. DOE, contract No. DEAC03-76SF00098.

### References

- [1] A. Rubio, J.L. Corkill, M.L. Cohen, *Phys. Rev. B (Condensed Matter)* 49 (1994) 5081.
- [2] R. Tenne, L. Margulis, M. Genut, G. Hodes, *Nature* 360 (1992) 444.
- [3] D. Golberg, Y. Bando, M. Eremets, K. Takemura, K. Kurashima, H. Yusa, *Appl. Phys. Lett.* 69 (1996) 2045.
- [4] D.P. Yu, X.S. Sun, C.S. Lee, I. Bello, S.T. Lee, H.D. Gu, K.M. Leung, G.W. Zhou, Z.F. Dong, Z. Zhang, *Appl. Phys. Lett.* 72 (1998) 1966.
- [5] G.W. Zhou, Z. Zhang, Z.G. Bai, D.P. Yu, *Solid State Commun.* 109 (1999) 555.
- [6] Z. Weng-Sieh, K. Cherrey, N.G. Chopra, X. Blase, Y. Miyamoto, A. Rubio, M.L. Cohen, S.G. Louie, A. Zettl, R. Gronsky, *Phys. Rev. B (Condensed Matter)* 51 (1995) 11229.
- [7] N.G. Chopra, R.J. Luyken, K. Cherrey, V.H. Crespi, M.L. Cohen, S.G. Louie, A. Zettl, *Science* 269 (1995) 966.
- [8] O. Stephan, P.M. Ajayan, C. Colliex, P. Redlich, J.M. Lambert, P. Bernier, P. Lefin, *Science* 266 (1994) 1683.
- [9] A. Loiseau, F. Willaime, N. Demoncey, G. Hug, H. Pascard, *Phys. Rev. Lett.* 76 (1996) 4737.
- [10] X. Blase, A. Rubio, S.G. Louie, M.L. Cohen, *Europhys. Lett.* 28 (1994) 335.
- [11] W. Han, Y. Bando, K. Kurashima, T. Sato, *Appl. Phys. Lett.* 73 (1998) 3085.
- [12] S. Iijima, *Nature* 354 (1991) 56.
- [13] R.S. Pease, *Acta Crystallogr.* 5 (1952) 356.
- [14] B.W. Smith, M. Monthieux, D.E. Luzzi, *Nature* 396 (1998) 323.
- [15] A. Thess, R. Lee, P. Nikolaev, H. Dai, P. Petit, J. Robert, C. Xu, Y.H. Lee, S.G. Kim, A.G. Rinzler, D.T. Colbert, G.E. Scuseria, D. Tomanek, J.E. Fischer, R.E. Smalley, *Science* 273 (1996) 483.
- [16] Y.-K. Kwon, Y.H. Lee, S.-G. Kim, P. Jund, D. Tomanek, R.E. Smalley, *Phys. Rev. Lett.* 79 (1997) 2065.
- [17] D.S. Bethune, C.H. Kiang, M.S. deVries, G. Gorman, R. Savoy, J. Vazquez, R. Beyers, *Nature* 363 (1993) 605.
- [18] S. Iijima, T. Ichihashi, *Nature* 363 (1993) 603.